Line Profile Analysis and Crystal Structure of Fibers

R Somashekar

Abstract | Line profile analysis, of X-ray diffraction data collected from samples like metal oxides, polymers, polymer blends and fibers (both man-made and natural), has become a common tool to obtain information of microstructure and lattice defects. Such analysis also have significant effect on the crystal structure of samples. Present review deals with various line profile analysis techniques including latest developments in the field and their application in crystal structure determination , especially in the case of fibers.

1. Introduction

Line profile analysis has been in general use for the investigation of the microstructure of crystalline materials since 1920[1]. For the peak shape analysis two fundamental different approaches that have been developed during the past four decades[2,3]. Of the two, Rietveld method has become a standard procedure except for the determination of microstructure. There are several attempts to incorporate the determination of microstructure in Rietveld method[4–7]. Normally, broadening of peak profile occurs due to two fundamentally different reasons: (i) The effect of crystallite size and (ii) the effect of lattice distortion. Later being dependent on the order of diffraction profile, there are various methods of separating these two effects from the peak profiles[8–12]. These are normally referred to as multiple order method. They can be used when there are Bragg reflections of the type (110), (220), (330),. . . etc. Here size broadening is caused by the finite number of unit cells in a column length of coherently scattering domains where this number of unit cells are counted in a direction normal to the Bragg planes.

Lattice distortion in a crystalline lattice can be described in two ways[13]. In the first kind, there is a certain probability that a lattice point is displaced from its mean position. However, away from the origin, the probability of a certain displacement from the mean position stays the same. Thus long range order is preserved. This is the kind of disorder caused by thermal vibrations of atoms/molecules and is called thermal or type I disorder. In the second kind, the length of the vectors joining the lattice points are distributed with a certain probability function. To construct a lattice, a vector is selected at random and laid down with one end at the origin. The location of the other end will have a certain probability distribution. A second vector is now selected and laid down with one end on the most probable end of the first. The other end will have a different wider probability distribution given by convolution of two functions. The length of the vector will have the same distribution. If this is continued, the probability of finding a lattice point at a certain distance equivalent to the crystallite size, from the origin, will be almost zero. The extent of change in the long range order, is the measure of lattice distortion or lattice strain expressed interms of percentage. This is called paracrystalline or type-2 disorder. In addition to these, the broadening are also caused by the presence of dislocation, stacking faults, grain boundaries, inclusions, precipitates etc.

2. Theoretical overview

The intensity profile, using the Fourier cosine series of the Warren and Averbach method[11,12] and Hosemann's one-dimensional paracrystalline

Department of Studies in Physics, University of Mysore, Manasagangotri, Mysore 570006, India
URL: http://faculty.physics.uni-mysore.ac.in/rs

rs@physics.uni-mysore.ac.in

Figure 1: X-ray diffraction pattern of silk fibers. (a) Hosamysore, (b) C.nichi, (c) PureMysore and (d) Nistari.

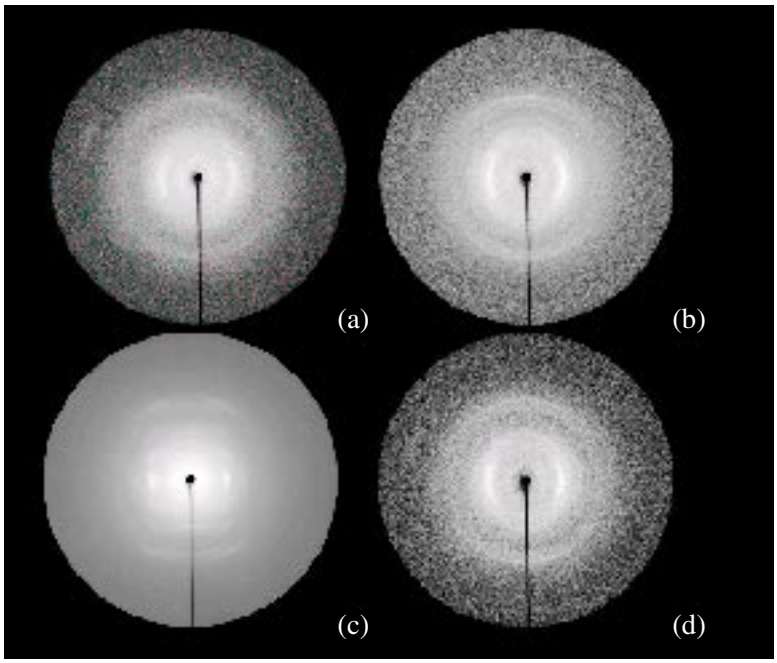

model[13] in a direction joining the origin to the center of the reflection, can be described as follows:

$$I(s) = \sum_{n=-\infty}^{\infty} A(n)\cos\{2\pi nd(s-s_o)\}, \qquad (1)$$

where the $A(n)$ are the harmonic coefficients that can be represented as a function of crystal size $\langle N\rangle$ and lattice distortion g, d is the inter planar spacing, $s = (\sin\theta)/\lambda$, s_o is the value of s at the peak of the reflection, θ is the Bragg angle, λ is the wavelength of the radiation and n is the harmonic number. The Fourier coefficients $A(n)$ of the profile are expressed as the convolution of crystal size $A_s(n)$ and lattice strain $A_d(n)$ coefficients as:

$$A(n) = A_s(n)\cdot A_d(n). \qquad (2)$$

Sometimes, this equation is also expressed in terms of variable $L = nd$, where d being the inter planar spacing and written as $A(L)$.

2.1. *Distortion effect*

The lattice distortion Fourier coefficients can be expressed in the following form[12]:

$$A_d(n) = \exp(-2\pi^2 m^2 n g^2) \qquad (3)$$

where m is the order of reflection and g is the lattice disorder $g(=\Delta d/d)$, which is also referred to as lattice strain. One also defines a mean square strain $\langle\epsilon^2\rangle$ which is given by $\frac{g^2}{n}$. This mean square strain is dependent on n, where as g is not[14,15]. Here $\langle\epsilon^2\rangle$ is the mean square strain depending on the displacement of atoms relative to their ideal positions and the angular brackets indicate spatial averaging.

2.2. *Crystal size effect*

For the calculation of the Fourier transform of the peak profile originating from a crystallite, we divide the crystal into cylindrical columns with N number of unit cells in a column. If $P(i)$ is the probability distribution function of column lengths, then, the crystallite size contribution to Fourier coefficients[16] is given by

$$A_s(n) = 1 - \frac{nd}{D} - \frac{d}{D}\left[\int_0^n iP(i)di - n\int_0^n P(i)di\right] \qquad (4)$$

where $D = \langle N\rangle d$, is the crystallite size. There are various functions and widely used methods to

Figure 2: X-ray diffraction pattern of silk-I modification

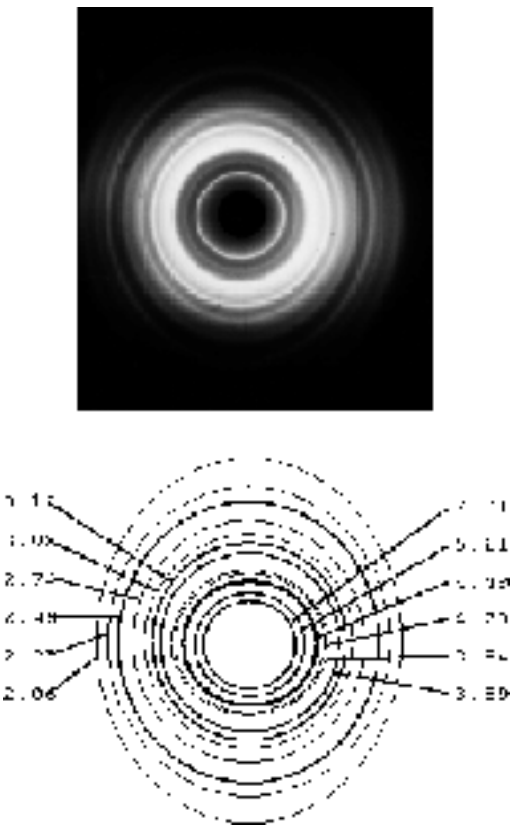

Figure 3: X-ray diffraction pattern of dch32 cotton fiber

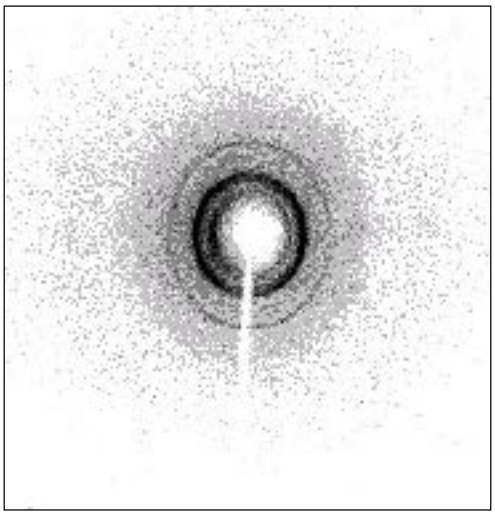

separate the strain and size components from the intensity profile and these are listed below.

2.2.1. *Ribarik, Ungar and Gubieza method:*

In this method, a Lognormal size distribution function given by[17]

$$P(i) = \frac{1}{(2\pi)^{1/2}} \frac{\sigma}{i} \exp\left\{ -\frac{[log(i/m)]^2}{2\sigma^2} \right\} \qquad (5)$$

Figure 4: Crystallite shape ellipsoid in silk-I modification

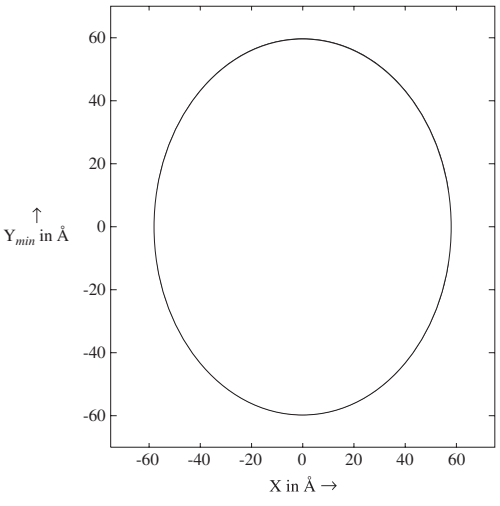

where σ is the variance and m is the median/width of the distribution, has been used in equation (4). The simplified equation has been used to compute microstructural parameters from diffraction profiles of materials with cubic or hexagonal crystal lattices. This is essentially multiple order method which has been efficiently used to compute the parameters of severely deformed copper and ball-milled lead sulfide specimens.

2.2.2. *Langford and Louer method:*

In this method, a least squares comparison of an experimental powder diffraction pattern with one generated from a physical model of various crystallite size distributions have been used in the case of samples of high symmetry[18,19].

2.2.3. *Whole Powder Pattern Modelling method of Scardi and Leoni[20]*

It is essentially a logical development of Langford work on pattern-decomposition methods based on the fitting of assumed analytical functions. Here, crystallites are assumed to be spherical and TEM data indicated that the distribution of diameters is closely Lognormal. The non-linear least-squares program MARQX developed by Dong and Scardi[21] finds the refined parameters of Lognormal distribution and results are in agreement with other integral breadth methods. Scardi has developed this approach and has demonstrated the viability of WPPM by including structural mistakes. WPPM is a major advance in line profile analysis which avoids the assumptions and approximations made in earlier procedures. The main factor affecting the reliability of the results is the validity of the physical models used to determine microstructure. Furthermore, this method is applicable to samples of high symmetry.

2.3. *Single order method: Fiber diffraction*

Several earlier investigators have proposed single order method and most of these methods rely heavily on low order coefficients[22–25]. A method is needed which avoids normalization and uses experimental coefficients of all harmonics taking into account the effect of truncation and error in background estimation. We describe here a method that meets these requirements and analyse the inescapable limitations imposed by unavoidable defects in the background corrected profile.

The techniques hither to described can be used for materials with high symmetry like metals and metal-oxide compounds, where more than two orders of reflection are available. In case of natural polymers like silk and cotton, it is rare to find multiple reflections and hence the techniques based

Figure 5: Crystallite shape ellipsoids in various silk fibers

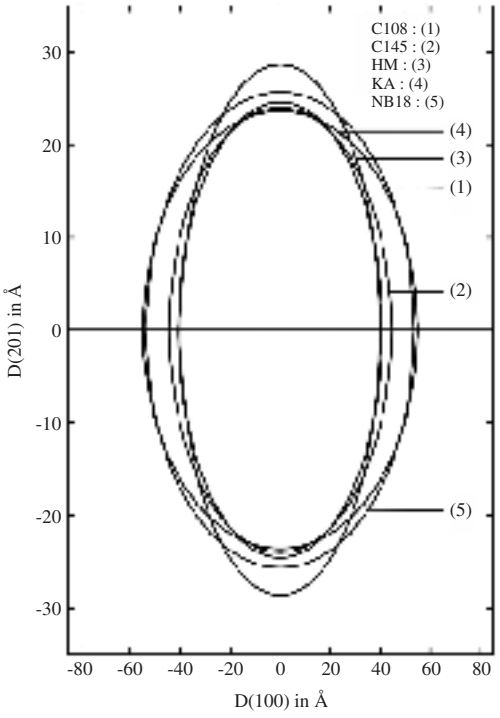

on Warren-Averbach method cannot be used. In this section, the technique where in single order method is used to obtain the crystallite size and lattice strain will be elucidated[16,26]. Essentially several asymmetric functions for $P(i)$ in equation (4) have been used to find the finer details of the microstructure of cotton/silk fibers. They are namely (i) Exponential, (ii) Reinhold and (iii) Lognormal functions. Substitution of these functions in equation (4) and carrying out simple integration, gives the size contribution to Fourier Coefficients. They are:

Exponential Distribution:

$$A_s(n) = \begin{cases} A(0)(1-\frac{n}{N}) & \text{if } n \le p \\ A(0)\exp\{-\alpha(n-p)\}/(\alpha N) & \text{if } n \rangle p \end{cases}$$

Here the distribution depends on no columns containing fewer than p unit cells and those with more than p will decay exponentially. The width of the distribution is given by $\alpha = \frac{1}{(N-p)}$.

Reinhold distribution:

$$A_s(n) = \begin{cases} A(0)(1-\frac{n}{N}) & \text{if } n \le p \\ \{A(0)(n-p+2/\beta)/N\} & \\ \exp\{-\beta/(n-p)\} & \text{if } n \rangle p \end{cases}$$

Here, β is the measure of width of the distribution.

Lognormal distribution[4]

$$A_s(n) = \frac{m_\alpha^3 \exp[(\frac{9}{4})(2^{1/2}\sigma^2]}{3} \text{erfc}\left[\frac{\log(n/m_\alpha)}{2^{1/2}\sigma} - (3/2)2^{1/2}\sigma\right] - m_\alpha^2 \frac{\exp(2^{1/2}\sigma)^2}{2} \times n\text{erfc}\left[\frac{\log(n/m_\alpha)}{2^{1/2}\sigma} - 2^{1/2}\sigma\right] + \frac{n^3}{6}\text{erfc}\left[\frac{\log(n/m_\alpha)}{2^{1/2}\sigma}\right] \quad (6), (7)$$

where σ and m_α are the variance and the median of the distribution function for the crystallite sizes.

From these, the area weighted number of unit cells in a column is given by

$$N_s = \frac{2m_\alpha \exp\left[(5/4)(2^{1/2}\sigma^2)\right]}{3} \quad (8)$$

and volume weighted number of unit cells in a column is given by

$$N_v = \frac{3m_\alpha \exp\left[(7/4)(2^{1/2}\sigma^2)\right]}{4}. \quad (9)$$

Table 1: Refinement parameters for silk I with $(Ala-Gly)_2-Ser-Gly$ repeating unit

	1	2
$\phi_{Ala-Ser}$	−112.09	−101.71
$\psi_{Ala-Ser}$	−5.55	−12.15
$\omega_{Ala-Ser}$	179.23	160.94
χ_{Ser}	174.64	167.85
ϕ_{Gly}	71.39	73.83
ψ_{Gly}	−98.66	−105.87
ω_{Gly}	−172.10	177.03
ϵ_x	14.50	0.23
ϵ_y	52.34	62.36
ϵ_z	−62.10	−49.15
$S(Å)$	−2.0077	−2.0073
$\mu(^o)$	90.29	90.27
w	0.0464	0.0464
1	2	
N1(Ala)–O2(Gly) (2.98,76.90)	N1(Ala)–O2(Gly) (2.85, 79.87)	
N2(Gly)–O1(Ala) (3.13,125.6)	N2(Gly)–O1(Ala) (2.87, 127.72)	
N1(Ala)–O1(Ala) (2.88, 86.4)	N1(Ala)–O1 (2.96, 79.95)	
O2(Ser)–O1(Ala) (2.65, 88.5)	O3(ser)–O1(Ala) (2.73, 86.83)	

1: without strain corrections
2: with strain corrections

Figure 6: Crystal structure with and without strain corrections in silk-I modification

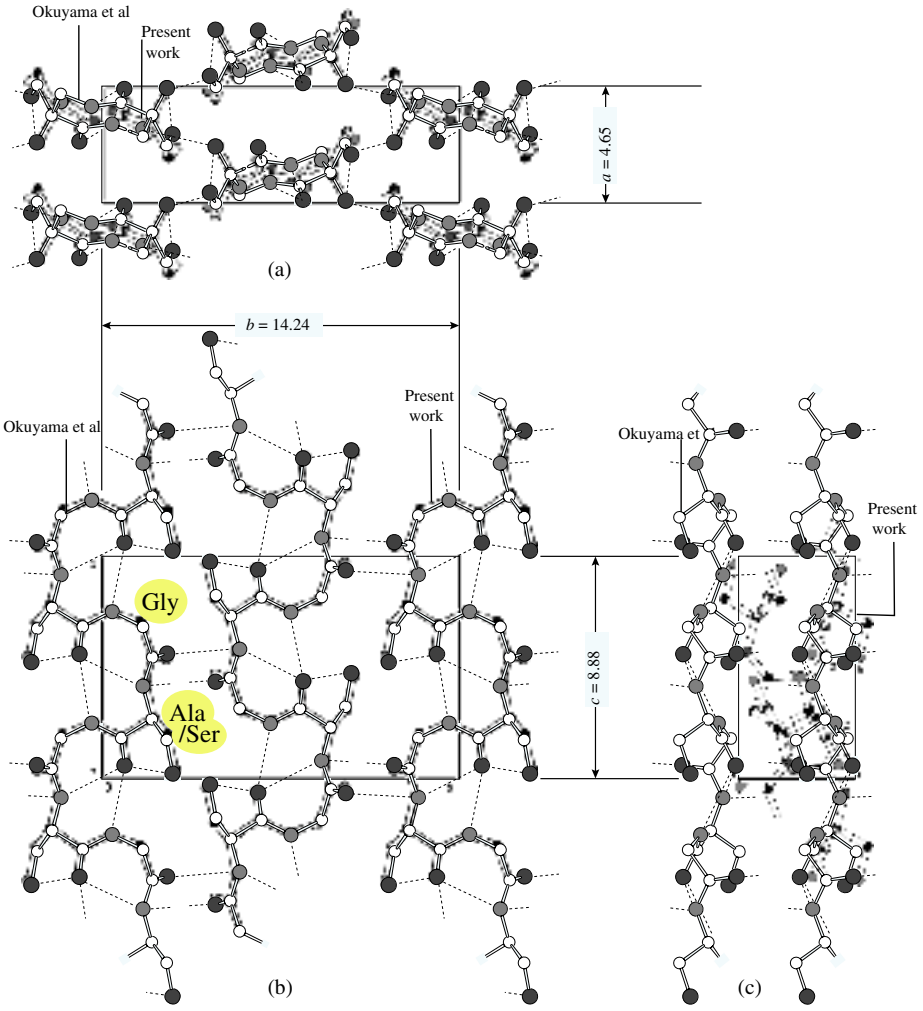

3. Computation of microstructure parameters in fibers

Illustrative X-ray recording patterns for some silk fibers used for computation are given in Figure 1. Figure 2 shows silk-I modification. Figure 3 shows cotton fiber X-ray diffraction photograph. The measured equatorial scan of the X-ray reflection profile intensities were corrected for Lorentz-Polarization factors and instrumental broadening using Stokes method[27]. Initial values of g and N were obtained using the method of Nandi et al.[25]. Substitution of these values in the equations mentioned earlier in the text, gives the corresponding for the width of distribution. These are only rough estimates, so that the refinement procedure must be sufficiently robust to start with such values. Here, we compute

$$\Delta^2 = [I_{cal} - (I_{exp} + BG)]^2 / npt, \qquad (10)$$

where BG is the error in the background estimation and npt is number of data points in a profile. The values of Δ were divided by half the maximum value of intensity so that it is expressed relative to the mean value of intensities and then minimised. For refinement against intensities using the above equations, a multidimensional minimization algorithm of the SIMPLEX method was used[28].

4. Crystallite shape in fibers

Crystallite sizes were determined using the above method for various Bragg reflections in silk and cotton fibers and they were projected onto a common plan by using the relation

$$\left(\frac{2}{N}\right)^2 = \left(\frac{\cos\theta}{Y}\right)^2 + \left(\frac{\sin\theta}{X}\right)^2 \qquad (11)$$

Figure 7: Crystal structure with strain corrections in dch32 cotton fibers.

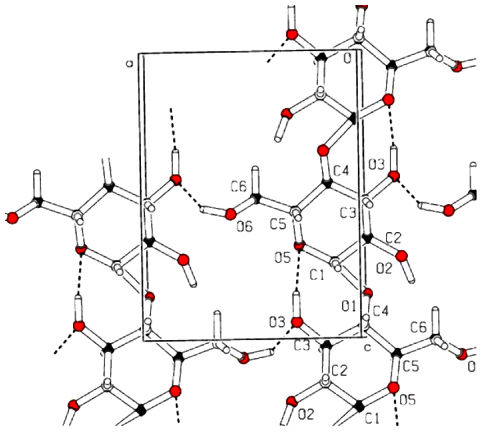

Figure 4(a–c) show crystallite ellipsoid in the case of silk-I modification, various raw silk fibers and cotton fibers.

5. Strain corrected intensity profiles and crystal structure in fibers

Having computed residual strains present in various fibers, these parameters were used to compute strain corrected integrated intensities of profiles in fibers. For this purpose, the crystal size parameters along with the width of the crystal size distribution function and the lattice strain were used to generate the strain corrected intensity profiles employing equations (1)–(3) and (6). Strain corrected intensities for the profiles were used to compute the crystal and molecular structure of these fibers like silk-I and cotton fibers.

5.1. *Molecular structure of silk-I*

To find the effect of residual strain corrections on the intensity profiles and hence crystal structure in silk-I modification, an hexapeptide $L-Ala-Gly-L-Ala-Gly-L-Ser-Gly$ model as a chemical repeating unit of the C_P fraction was used for the analysis. Molecular models having the appropriate helical symmetry and fiber repeating period were generated using LALS method[29–31] with all standard bond lengths and angles held constant. The molecular structure of the silk fibroin in silk-I modification has 2/1 helical symmetry. The value of dihedral angles (ϕ, ψ) of Glycin and Alanin residues were taken from the results of earlier investigation.

The most possible space group and the number of chemical repeating unit of $L-Ala-Gly$ in a unit cell were determined to be $P2_12_12_1$ and four respectively. The details of computation involving LALS method is given in an earlier paper[32]. The main aim of including the strain correction was to find out the molecular conformational changes due to residual strain and hence to identify the reason for mechanical instability of silk-I modification. Crystal and molecular structure of silk-I with and without residual strain corrections are given in Figure 5.

Although not much change in the conformation of molecules down the *a*- and *b*-axes are visible in the diagram, there seems to be significant change in the molecular arrangement in the *ab*-plane. This change in *ab*-plane enhances the fragility of the silk-I modification, which results in easier transition to silk-II modification despite reasonable hydrogen bond network. The sterochemical energy computed in LALS method corresponding to the final crystal structure by including residual strain corrections has a low value which indicates the stability of structure and packing of the molecules in the unit cell. Various molecular parameters obtained for silk-I modification with and without strain corrections are tabulated in Table 1.

5.2. *Molecular structure of cotton fibers*[33]

Cellulose is a polymer of D-glucopyranose in which pyranose rings are linked by $\beta(1-4)$ glucosidic linkages, with the pyranose ring taking the chair conformation, which is the most probable conformation in the solid state. Molecular models having the 2/1 helical symmetry and a fiber repeating period of 10.34 Å, together with the pyranose ring in the molecular model was constructed and used as an input for the LALS program with standard bond lengths and angles. The computation of molecular structure in a unit cell using LALS was carried out in two steps. First with experimental integrated intensities without strain corrections and second with the microstructural parameters being used to incorporate strain correction and then using integrated intensities in LALS program. A map of molecular and crystal structure of strain corrected cotton fiber was plotted using "PLATON"[34] and given in Figure 5. It is observed that by incorporating strain corrected integrated intensities, there are fractional changes in the bond angles and bond lengths for the cotton interms of cellulose chains which certainly affect crystal volume. It is note worthy to mention that the changes are less significant when compared to disordered systems such as alloys. The changes that are observed in the molecular parameters with and without strain corrections for the profiles of dch32 cotton fiber are given in Table 2.

Table 2: Model molecular parameters for dch32 cotton fibers with and without strain corrections.

	With strain correction	Without strain correction
Torsion angles and bond angles at glycosidic linkage(deg)		
$\phi(C2-C1-O1-C'4)$	(no change)	146.98±0.30
$\psi(C1-O1-C'4-C'3)$	(no change)	61.01±0.12
$\tau(C1-O1-C'4)$	(no change)	113.34±0.23
Orientation of O6 (deg)		
$\chi(O5-C5-C6-O6)$	88.84±0.18	88.37±0.17
Packing parameters of polymer chains		
$\mu 1^a$	104.54±0.21	104.52±0.21
$w1^b$	0.635±0.001	0.639±0.001
$\mu 2^a$	92.24±0.10	92.14±0.18
$w2^b$	0.374±0.001	0.378±0.001
Scale factor[c]	0.160±0.003	0.167±0.003
Attenuation factor[d]	−24.46±0.05	−23.26±0.05
R^e	0.189±0.003	0.189±0.003
R_w^e	0.235±0.003	0.226±0.003

[a] $\mu 1$ and $\mu 2$ are the azimuth angles for two separated chains around their molecular axis.
[b] $w1$ ans $w2$ are the heights of the origin atoms for the separated chains along c-axis.
[c] Scale factor is the factor by which the calculated intensities should be multiplied to bring the magnitude within the range of experimental data.
[d] Attenuation factor is the amount of absorption of the radiation by the atoms.
[e] R and R_w are the normal and weighted residual factors.

6. General observation

Microstructure parameters are computed by line profile analysis by assuming simple analytical function. Undoubtedly whole powder pattern modelling (WPPM) is the best approach for samples like metal-oxides with high symmetry. If finer details of microstructure are required, then neither size nor the strain profiles can be approximated by simple analytical functions. WAXS analysis of profiles in fibers like silk and cotton can be done with single order methods which are proven to give good reliable results[35]. Further, structure analysis using these strain parameters, to correct integrated intensities, indicate changes in bond lengths, bond angles and molecular packing within unit cell in the case of silk-I and cotton fibers which results in a more stable structure.

Received 14 June 2007; revised 18 July 2007.

References

1. K. Becker, Z. Phys. **42**, 226 (1927).
2. H. M. Rietveld, Acta.Cryst. **22**, 15 1 (1967).
3. L. MeCuster, R. B. V. Dreele, D. Cox, D. Louer, and P. Scardi, J. Appl. Cryst. **32**, 36 (1999).
4. T. Ungar, M. Leoni, and P. Scardi, J. Appl. Cryst. **32**, 290 (1999).
5. P. Scardi and M. Leoni, J. Appl. Cryst. **32**, 671 (1999).
6. J. I. Langford, D. Louer, and P. Scardi, J. Appl. Cryst. **33**, 964 (2000).
7. I. Lucks, P. Lamparter, and E. J. Mittemeijer, J. Appl. Cryst. **37**, 300 (2004).
8. A. J. C. Wilson, Acta. Cryst. **11**, 227 (1958).
9. E. F. Bertaut, Acta. Cryst. **3**, 14 (1950).
10. G. K. Williamson and W. H. Hall, Acta. Metall. **1**, 22 (1953).
11. B. E. Warren and B. L. Averbach, J. Appl. Phys. **23**, 491 (1952).
12. B. E. Warren, Prog. Met. Phys. **8**, 147 (1959).
13. R. Hosemann, Z. Phys. 128, 465 (1950).
14. R. L. Rothman and J. B. Cohen, Adv. X-ray. Anal **12**, 208 (1969).
15. R. Somashekar, Chapter 30, Defect and Microstructure Analysis by diffraction; Eds R. L. Snyder, J. Fiala and H. J. Bunge, IUCr Monograph p. 728 (1999).
16. I. H. Hall and R. Somashekar, J. Appl. Cryst. **24**, 1051 (1991).
17. G. Ribarik, T. Ungar, and J. Gubieza, J. Appl. Cryst. 34, 669 (2001).
18. J. I. Langford and D. Louer, Rep. Prog. Phys. **59**, 131 (1996).
19. J. I. Langford, D. Louer, and P. Scardi, J. Appl. Cryst. **33**, 964 (2000).
20. P. Scardi and M. Leoni, Acta. Cryst. (A) **58**, 190 (2001).
21. Y. H. Dong and P. Scardi, J. Appl. Cryst. **33**, 184 (2000).
22. A. Gangulee, J. Appl. Cryst. **7**, 434 (1974).
23. J. Mignot and D. Rondot, Acta. Metall. **23**, 1321 (1975).
24. M. Zocchi, Acta. Cryst. **A36**, 164 (1980).
25. R. K. Nandi, H. R. Kuo, M. Schlosborg, G. Wissler, J. B. Cohen, and J. B. Crist, J. Appl. Cryst. **17**, 22 (1984).
26. R. Somashekar, I. H. Hall, and P. D. Carr, J. Appl. Cryst. **22**, 363 (1989).
27. A. R. Stokes, Proc. Phys. Soc. Lond. **61**, 382 (1948).
28. W. Press, B. P. Flannery, S. Teukolsky, and W. T. Vetterling, Numerical Recipes Cambridge University Press (1986).
29. K. Okuyama, R. Somashekar, K. Noguchi, and S. Ichimura, Biopolymer **59**, 310 (2001).
30. Y. Sangappa, K. Okuyama, and R. Somashekar, J. Appl. Poly. Sci. **91**(5), 3045 (2004).
31. P. J. Smith and S. Arnott, Acta. Cryst. **34**, 3 (1978).
32. Y. Sangappa, S. S. Mahesh, and R. Somashekar, J. Bioscience. **12**, 465 (2005).
33. O. M. Samir and R. Somashekar, Powder Diffraction **22**(1), 20 (2007).
34. A. L. Spek, J. Appl. Cryst. **36**, 7 (2003).
35. D. Balzar, N. Audebran, M. R. Daymond, A. Fitch, A. Hewat, J. I. Langford, A. LeBail, D. Louer, O. Masson, C. N. McCowan, et al., J. Appl. Cryst. **37**, 911 (2004).

Dr R Somashekar is a professor at Department of Studies in Physics, University of Mysore, Manasagangotri, Mysore. He was a research associate at Department of Pure and Applied Physics, UMIST, Manchester, UK and also visiting professor under JSPS of Japan at Tokyo University of Agriculture and Technology(TUAT), Tokyo, Japan. He has developed single order method of line profile analysis and has contributed a chapter on this topic in International Union of Crystallography monograph. Professor Somashekar's research is focused on characterisation of materials interms of microstructure parameters to understand the structure-property relation in these materials. He has authored more than 150 research papers in National and International journals.